

# Model-Based Registration for Dynamic Cardiac Perfusion MRI

Ganesh Adluru, BE,<sup>1,2</sup> Edward V.R. DiBella, PhD,<sup>2,3\*</sup> and Matthias C. Schabel, PhD<sup>2</sup>

**Purpose:** To assess the accuracy of a model-based approach for registration of myocardial dynamic contrast-enhanced (DCE)-MRI corrupted by respiratory motion.

**Materials and Methods:** Ten patients were scanned for myocardial perfusion on 3T or 1.5T scanners, and short- and long-axis slices were acquired. Interframe registration was done using an iterative model-based method in conjunction with a mean square difference metric. The method was tested by comparing the absolute motion before and after registration, as determined from manually registered images. Regional flow indices of myocardium calculated from the manually registered data were compared with those obtained with the model-based registration technique.

**Results:** The mean absolute motion of the heart for the short-axis data sets over all the time frames decreased from  $5.3 \pm 5.2$  mm ( $3.3 \pm 3.1$  pixels) to  $0.8 \pm 1.3$  mm ( $0.5 \pm 0.7$  pixels) in the vertical direction, and from  $3.0 \pm 3.7$  mm ( $1.7 \pm 2.1$  pixels) to  $0.9 \pm 1.2$  mm ( $0.5 \pm 0.7$  pixels) in the horizontal direction. A mean absolute improvement of 77% over all the data sets was observed in the estimation of the regional perfusion flow indices of the tissue as compared to those obtained from manual registration. Similar results were obtained with two-chamber-view long-axis data sets.

**Conclusion:** The model-based registration method for DCE cardiac data is comparable to manual registration and offers a unique registration method that reduces errors in the quantification of myocardial perfusion parameters as compared to those obtained from manual registration.

**Key Words:** dynamic MR; cardiac perfusion; motion correction; registration; respiratory motion; compartment models

**J. Magn. Reson. Imaging 2006;24:1062–1070.**  
© 2006 Wiley-Liss, Inc.

DYNAMIC MR EVALUATION of myocardial perfusion is becoming a powerful tool for the detection of coronary artery disease (1–3). The standard approach is to rapidly acquire T1-weighted images to track the uptake and washout of the contrast agent Gd-DTPA. Multiple 2D images are acquired each heartbeat. The slices are acquired using ECG-gated sequences so that a given slice is always acquired during the same phase of the cardiac cycle. The time-series data are analyzed visually or with semiquantitative or quantitative models (4,5). Depending on the analysis technique used, at least 20–40 seconds of data are needed to determine regional perfusion values in the left ventricular (LV) myocardium. Many patients cannot hold their breath long enough to provide a motion-free study. A breath-hold of any appreciable length becomes more difficult when pharmacological stress is induced by vasodilating agents, which is necessary for detection of coronary artery disease. Respiration causes motion of the heart, which makes qualitative visual analysis difficult and can cause incorrect estimation of semiquantitative and quantitative parameters.

A number of registration methods have been proposed to correct the motion of the heart in dynamic contrast MRI acquisitions (6–10). In the method of Bidaut and Vallee (6), the mean squared difference between images in the perfusion sequence and a reference image in a region defined by a cardiac mask is minimized. The initial reference image is chosen to be an early image from the perfusion sequence, which does not show any contrast agent. After all of the frames are registered to the reference frame, the reference image is updated iteratively by taking the average of all of the registered images in the previous iteration. Gallippi et al (7) correct for motion using a statistical approach whereby an image in the temporal center of the sequence is chosen as the reference, and the images are registered using a matching metric based on intensity variations and edge directions. Dornier et al (8) minimize the mean squared difference proposed in (9) between the perfusion images within tightly cropped myocardial masks. Bracoud et al (10) use the mutual information (11) metric to register. The above methods register the perfusion images to a single reference image, which may not give the best results since contrast can vary greatly between the images. This was partly taken into account in the study by Bidaut and Vallee

<sup>1</sup>Electrical and Computer Engineering Department, University of Utah, Salt Lake City, Utah, USA.

<sup>2</sup>UCAIR, Department of Radiology, University of Utah, Salt Lake City, Utah, USA.

<sup>3</sup>Department of Bioengineering, University of Utah, Salt Lake City, Utah, USA.

\*Address reprint requests to: E.D., Utah Center for Advanced Imaging Research (UCAIR)/Radiology, 729 Arapeen Dr., Salt Lake City, UT 84108. E-mail: ed@ucair.med.utah.edu

Contract grant sponsor: NIH/NIBIB; Contract grant number: R01 EB000177.

Received October 5, 2005; Accepted July 28, 2006.

DOI 10.1002/jmri.20756

Published online 9 October 2006 in Wiley InterScience (www.interscience.wiley.com).

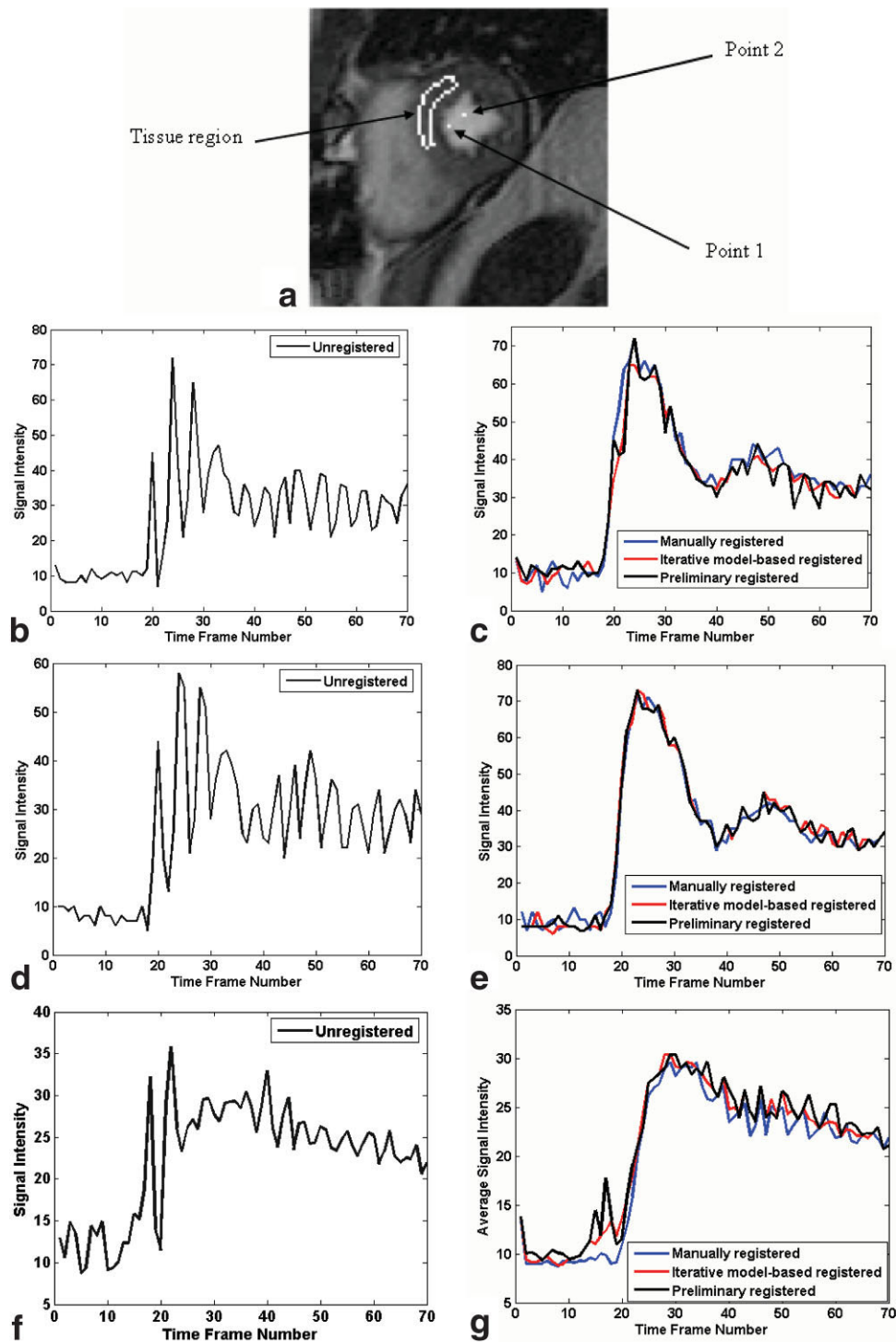


**Figure 1.** **a:** Tissue region and two points in the LV blood pool of a typical patient (patient 1) for comparing the SI time curves before and after registration. **b:** SI time curve for point 1 shown in image a in unregistered images. **c:** Comparison of SI time curves for point 1 shown in image a in manually registered, preliminary registered, and iterative model-based registered images. **d:** SI time curve for point 2 shown in image a in unregistered images. **e:** Comparison of SI time curves for point 2 shown in image a in manually registered, preliminary registered, and iterative model-based registered images. **f:** Average SI time curve for the tissue region shown in image a in unregistered images. **g:** Comparison of average SI time curves for the tissue region shown in image a in manually registered, preliminary registered, and iterative model-based registered images.

(6), in which an average reference frame was updated iteratively; however, a better strategy might be to perform the registration with multiple reference frames.

Recently Stegmann et al (12) proposed the use of active-appearance models to register the perfusion im-

ages. The active-appearance models capture the shape variability of the heart from a representative training set and use the models to fit the new perfusion images and register them. Generating the models involves extraction of shape contours of the objects of interest and

definition of landmark correspondences across the set of contours from the training data sets. This type of method, which is based on spatial features of the perfusion images, may perform poorly on some frames due to noise and the lack of well-defined features in some frames.

We propose an iterative model-based registration method based on a temporal parametric model for each pixel. The method uses the minimization of the mean squared difference, with a spatial weighting, to register each image in the perfusion sequence to its corresponding “model image” instead of registering all the images to a single reference image. This process is iterated to yield improved registrations. A similar idea was recently proposed for application to dynamic contrast-enhanced (DCE)-MRI tumor data (13).

## MATERIALS AND METHODS

### Data Acquisition

Perfusion data were acquired from 10 patients on Siemens Trio 3T or Siemens Avanto 1.5T scanners with a multi-element coil designed for cardiac imaging. Informed consent from the patients was obtained in accordance with the University of Utah Institutional Review Board. Using a saturation-recovery turbo fast low-angle shot (FLASH) sequence, three to four short-axis slices and one long-axis slice were acquired for different patients to follow the uptake of the contrast agent Gd-DTPA. The Gd-DTPA doses for different studies varied from 0.025–0.1 mmol/kg and were injected at a rate of 6 mL/second. The patients were instructed to hold their breath at end-expiration for as long as possible during the contrast uptake and to breathe shallowly thereafter. The parameters for the scans were TR ~ 2 msec; TE = 0.95–1.28 msec; TI ~ 100 msec; FOV = (255–380) × (192–285) mm<sup>2</sup>; and slice thickness = 7–8 mm. The acquisition matrix for different scans varied between 160 × 96 and 192 × 72. The reconstructed pixel size varied between 1.6 and 2.0 mm for different scans.

### Preprocessing

The acquired data contain a lot of motion of the heart (as high as 2.5 cm) due to respiration. Most of the motion in the data sets appears to be in-plane, although a few images have out-of-plane motion. Handling out-of-plane motion is a challenging problem that cannot be corrected postacquisition with current acquisition methods, and is not considered in this work. The motion of the heart is observed to be predominantly a rigid translation. A few frames have small rotational motion, which is not modeled for this work.

A rectangular mask that roughly encompasses the heart is first defined. The mask is large enough to include the heart in all of the images in the sequence. The binary mask is multiplied with all of the images to remove unwanted objects, such as the chest wall, which can move in a direction different from the heart.

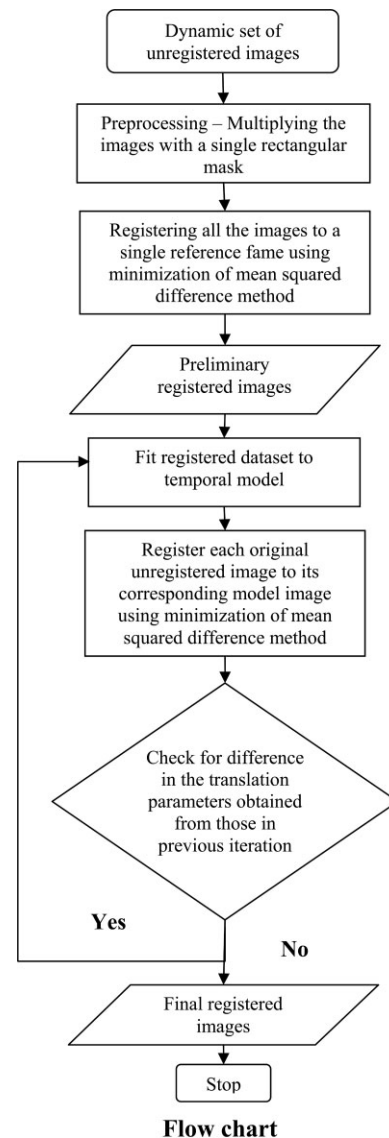


**Figure 2.** Flow chart for the iterative model-based registration algorithm.

### Model-Based Method

The main idea of the model-based method is to make use of the fact that for perfectly registered perfusion images, the signal intensity (SI) time curves for each pixel are relatively smooth in time. Motion typically causes the time curves to have outliers (for example, see the time curves for the points in the LV blood pool and those for the tissue region in an unregistered and registered data set in Fig. 1a–g). Thus a smooth “fit” to the curve can provide a measure of motion by identifying outliers. Models with a large number of parameters can fit time curves with even large amounts of motion well, defeating the idea of model-based registration by overfitting. To achieve a balance between smoothness and overfitting, a two-compartment model (14) is used to fit the data. Other models, such as the B-splines in Ref. 15, could possibly be used instead. The basic form of the two-compartment model is given by

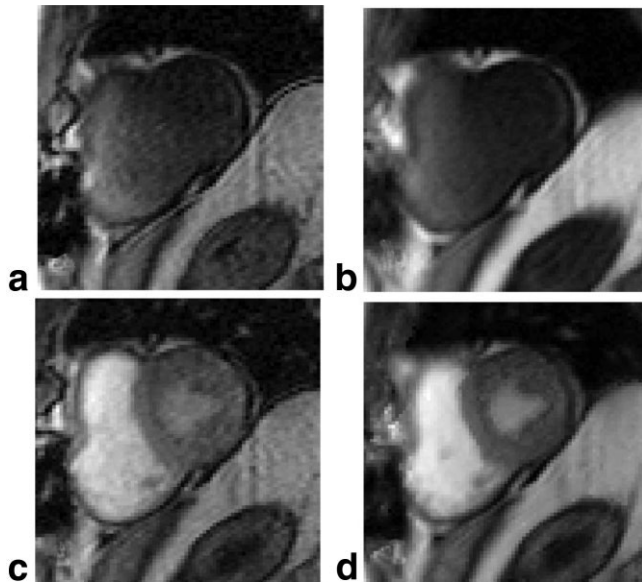


**Figure 3.** **a:** Original precontrast frame from the perfusion sequence for a typical patient (patient 1, cropped). **b:** Model image for the corresponding precontrast frame in a. **c:** Original postcontrast frame from the perfusion sequence for a typical patient (patient 1). **d:** Model image for the corresponding postcontrast frame in c.

$$\frac{dC_{pix}(t)}{dt} = K^{trans}C_{input}(t) - k_{ep}C_{pix}(t)$$

Since the model “expects” gadolinium (Gd) concentration curves, the SI time curves for each pixel are converted to be proportional to Gd concentration time curves by subtracting the precontrast signal, which is the average SI of approximately eight precontrast frames from each curve. In Eq. [1],  $C_{pix}(t)$  is this signal

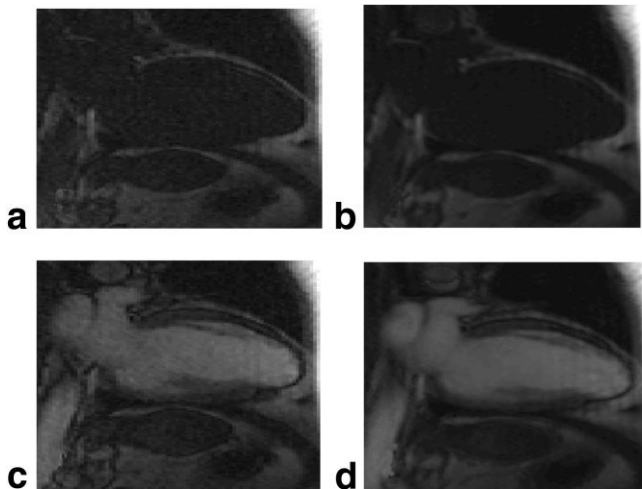


**Figure 4.** **a:** Original precontrast frame from the perfusion sequence for a typical two-chamber-view long-axis data set (cropped). **b:** Model image for the corresponding precontrast frame in a. **c:** Original postcontrast frame from the perfusion sequence for a typical two-chamber-view long-axis data set. **d:** Model image for the corresponding postcontrast frame in c.

Table 1  
Comparison of Average Absolute Motion in Vertical (Y) and Horizontal (X) Directions Before and After Registration for a Typical Short Axis Slice with 70 Frames from a Patient (Patient #1)\*

Registration method	Mean ± SD of the absolute translation in Y (mm)	Mean ± SD of the absolute translation in X (mm)
Unregistered	3.9 ± 3.8	4.6 ± 3.6
Preliminary registered	1.8 ± 1.7	2.9 ± 2.5
Iterative model-based	1.2 ± 1.1	2.5 ± 1.7

\*Pixel size = 1.8 mm.

difference time curve for each pixel, and  $C_{input}(t)$  is the input function that is chosen as the average of the signal difference time curves in a small region in the right ventricular (RV) blood pool. The parameters  $K^{trans}$  and  $k_{ep}$  are the rate constants for the exchanges of contrast agent between plasma and the extravascular extracellular space [16].

This type of model is widely used in DCE-MRI. Including a vascular term and time delay in Eq. [1] gives

$$\frac{d}{dt}[C_{pix}(t) - v_p C_{input}(t - \tau)] = K^{trans}C_{input}(t - \tau) - k^{ep}[C_{pix}(t) - v_p C_{input}(t - \tau)]$$

where  $v_p$  and  $\tau$  represent blood volume per unit volume of tissue and time delay in the input function, respectively. Each modified signal difference time curve is modeled according to Eq. [2].

It is computationally intensive to use the standard method of fitting the solution of Eq. [2] in the model-based registration approach. The standard solution of Eqs. [1] and [2] is obtained by convolving the input

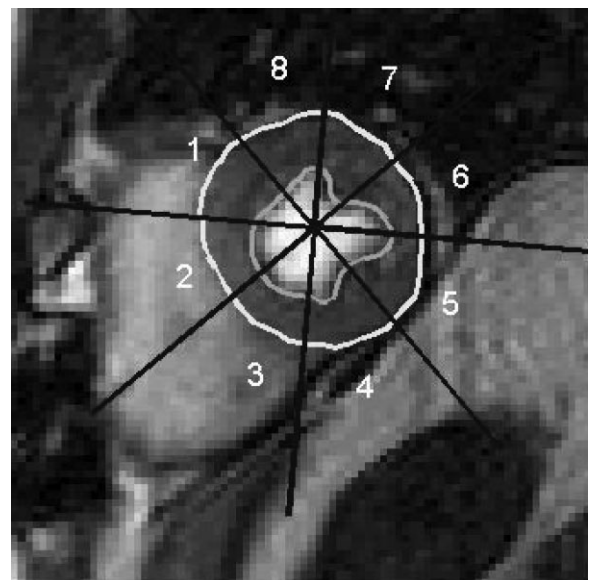


**Figure 5.** The myocardium is divided into eight regions to estimate the flow indices by performing a two-compartment model analysis for a typical patient (patient 1).

function  $C_{input}$  with a decaying exponential. Each pre-processed image has on the order of 10,000 pixels, and each pixel has a time curve of approximately 70 points. Since every pixel must be fit multiple times to evaluate different shifts in X and Y, it can be relatively slow to use the standard solution. A more rapid fitting method was recently used for MRI (17), and has been used for positron emission tomography (PET) (18). In this method, the problem is linearized by integrating both sides of Eq. [2], which is given by

$$C_{pix}(t) = (K^{trans} + k^{ep}v_p) \int_0^t C_{input}(\mu - \tau) d\mu - k^{ep} \int_0^t C_{pix}(\mu) d\mu + v_p C_{input}(t - \tau)$$

The parameters in Eq. [3] are chosen such that the chi-squared error between the fit and the original curves is minimized. This form without the time delay term (17) is much faster than standard nonlinear least squares. In application to dynamic cardiac MRI data, the delay  $\tau$  is critical for providing reasonable fits for different regions. For example, fitting the time curve for a pixel in the LV blood pool requires a delay of the RV input function for accurate representation.

To include the time delay  $\tau$ , Eq. [3] is solved rapidly with a matrix inversion to obtain the three parameters  $K^{trans}$ ,  $k_{ep}$ , and  $v_p$ , while the time delay  $\tau$  is held fixed. A first approximation of the time delay is obtained by using a coarse one-dimensional search grid and recomputing the three fit parameters  $K^{trans}$ ,  $k_{ep}$ , and  $v_p$  at each delay value. The grid is then made finer to find the optimal delay value that produces the best fit to the data. The model representation of the dynamic images is then generated by replacing each time curve with the parameterized curves obtained as above and adding back the precontrast signal.

The implementation of the model-based registration method is summarized by the flow chart in Fig. 2. After the preprocessing masking step, a relatively conventional initial registration is performed. This initial registration reduces the amount of blurring in the subse-

Table 2  
Comparison of Flow Indices for the Eight Regions Shown in Fig. 5 Obtained by Performing Two-Compartment Model Analysis Before and After Registration (Patient #1)

Region	Flow indices manually registered	Flow indices unregistered	Flow indices preliminary registered	Flow indices iterative Model-based
1	0.85	1.19	1.11	1.04
2	0.99	0.48	1.14	1.09
3	1.16	0.61	1.04	1.14
4	1.03	1.35	0.78	0.96
5	0.86	1.18	0.73	0.83
6	0.81	1.11	0.71	0.65
7	0.51	1.15	0.61	0.55
8	0.66	1.29	0.71	0.66

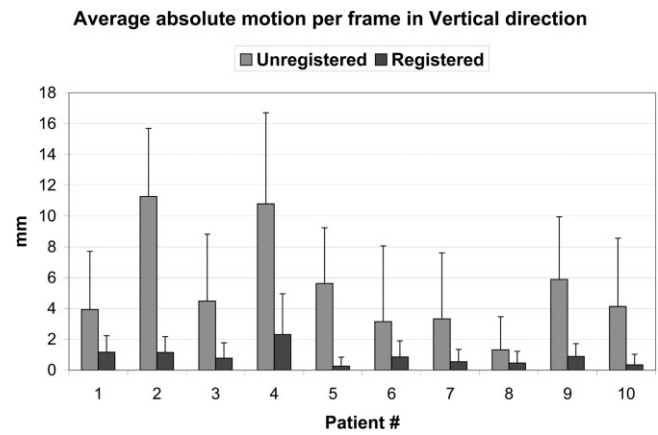


Figure 6. Comparison of the average absolute motion (mm) of the heart over all the time frames for short-axis slices from 10 patients before and after registration in the Y (vertical) direction.

quently generated model images caused by pixels with highly varying intensities due to motion. This initial registration is done by registering all of the original dynamic images to a single reference frame. The reference frame is chosen to have good contrast between the myocardium and the ventricle blood pools, as well as sufficient contrast uptake for some definition of the epicardium. Registration is done by minimizing the mean square difference between the reference image and all of the other perfusion images. For each image frame, a 2D raised cosine function, the Hanning window, is used to weight the squared differences. The Hanning window penalizes the square of the intensity difference in the center region more than in the outer regions of the image. The weighting function was chosen empirically from several different weighting functions, and made a substantial difference for some of the data.

Model images are then generated as outlined above using the preliminary registered images. Figure 3

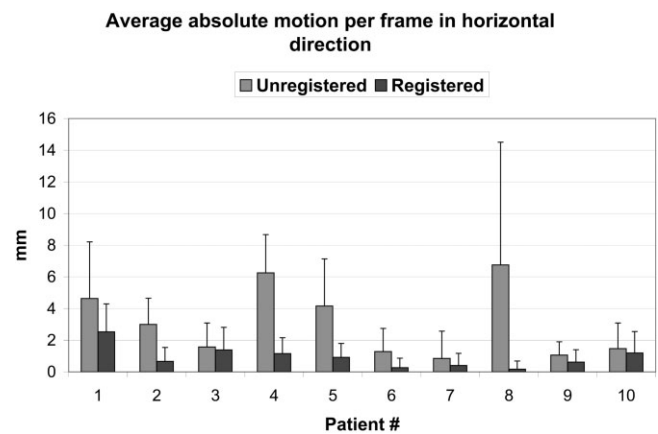
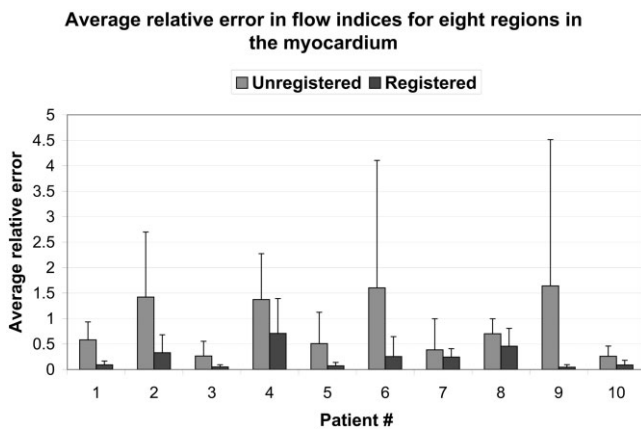


Figure 7. Comparison of the average absolute motion (mm) of the heart over all of the time frames for short-axis slices from 10 patients before and after registration in the X (horizontal) direction.



**Figure 8.** Comparison of the average relative error in the flow indices for the eight tissue regions before and after registration for short-axis slices from 10 patients.

shows the model images and the corresponding original images in a typical data set.

Each original unregistered image in the perfusion sequence is then registered with its corresponding model image by minimizing their mean square difference, with the spatial weighting (i.e., Fig. 3a is registered with Fig. 3b as the reference image, Fig. 3c is registered with Fig. 3d as the reference image, and so on). The above method is iterated. After a few iterations, no significant change occurs in the fits to the time curves of the pixels, and hence the reference images in the current iteration and those in the previous iteration are not very different. Consequently, when the unregistered images are registered to the reference images in the current iteration, the translation parameters obtained in X and Y directions for each unregistered frame are the same as those obtained in the previous iteration. That is, the algorithm is repeated until there are no changes in the translation parameters obtained in X and Y directions in the current and previous iterations for all the image frames.

Ten short-axis perfusion data sets (five rest perfusion and five adenosine stress perfusion), with 60–100 time frames each, are processed with the iterative model-based registration algorithm. Each of the 10 data sets is derived from a different patient. Seven are from patients being evaluated for coronary artery disease, and three are obtained from normal volunteers.

In addition, the algorithm is tested on 10 two-chamber-view long-axis perfusion data sets. The long-axis data sets are obtained from seven different patients. Long-axis images can contain other structures, such as the atrial blood pools. It is important to assess whether the model used in the model-based registration method can repre-

sent such features. Also, since the RV does not appear in the images, a different input function must be chosen. The input function  $C_{input}$  used in Eq. [3] to generate the model images is obtained in the same way as for the short-axis slices, but from a region chosen in the LV blood pool of the heart. Figure 4 represents the model images for a typical long-axis data set.

**Analysis**

Motion is estimated to the nearest pixel manually for each frame using custom software with user-drawn contours. The shifts obtained using manual registrations are compared with those obtained using the automatic method, and the reduction in motion is estimated. The percentage

improvement in motion is calculated as  $\left(1 - \frac{M_R}{M_{UR}}\right) \times 100\%$ , where  $M_R$  is the absolute measure of motion present after registration, and  $M_{UR}$  is the absolute of motion present before registration, assuming that the manually registered images are free of motion.

In addition, the myocardium is divided into regions of interest (ROIs) and a kinetic analysis with a two-compartment model is performed to determine the blood flow indices. This is the  $K^{trans}$  parameter in Eqs. [1]–[3]. The division of the tissue into regions is done on a single frame and the same regions are used for all of the frames. The flow indices calculated for manually registered images are compared with those from automatically registered data. The percentage improvement in the estimation of perfusion indi-

ces is calculated according to  $\left(1 - \frac{E_R}{E_{UR}}\right) \times 100$ , where  $E_R$

is the average absolute value of the differences in the perfusion flow indices between automatically registered and manually registered images, and  $E_{UR}$  is the absolute value of the difference in perfusion flow indices between unregistered and registered images. The average relative error of the flow indices is defined as  $E_R$  divided by the flow values from the manually registered images. Paired *t*-tests with Bonferroni correction are used to compare the flow values at a significance level of  $P < 0.05$ .

**RESULTS**

The complete results for a short-axis slice from a typical patient (patient 1) with 70 time frames are presented in Figs. 1, 3, 5, and Tables 1–2. Table 1 compares the average absolute motion for each image frame in the X and Y directions before and after registration. There is an improvement of 71% in registration by using the iterative model-based method as compared to an improvement of 54% after preliminary registration using a single reference image for the absolute mean shifts in the vertical or Y direction. An improvement of 46% is

**Table 3**  
Comparison of Flow Indices of the Regions in the Myocardium Before and After Registration for the 10 Short Axis Slices from 10 Patients Using Paired *t*-Tests with Bonferroni Correction

Paired <i>t</i> -tests with Bonferroni correction for flow indices	Manually registered vs. unregistered	Iterative model-based vs. unregistered	Manual registration vs. iterative model-based registration
<i>P</i>	0.00066	0.00093	1

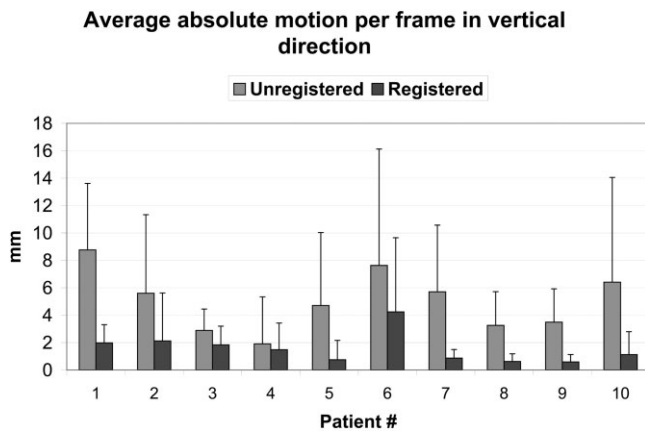


**Figure 9.** Comparison of the average absolute motion (mm) of the heart over all of the time frames for 10 two-chamber long-axis data sets before and after registration in the Y (vertical) direction. Negligible motion is observed in the X direction and is not shown.

observed using the iterative model-based method as compared to a 36% improvement after preliminary registration for the absolute mean shifts in the horizontal or X direction. Figure 1a–g shows two points chosen in the LV blood pool and a region in the tissue, and compare the respective SI time curves before and after registration.

In Fig. 5 the division of the myocardium into eight ROIs is shown. Table 2 compares the flow indices for each of the eight regions. The flow indices are obtained by performing a separate two-compartment model analysis before and after registration. The input function is obtained by subtracting the precontrast intensity for approximately eight frames from the average of SI time curves for a region in the LV blood pool. There is a total absolute improvement by 68% in the estimation of flow indices of eight regions after preliminary registration, and 83% improvement after using the iterative model-based method as compared to those from the manual registration.

The results for all 10 short-axis slices from 10 different patients are summarized in Figs. 6–8. Typically, three to five iterations are required before registration is completed. The average absolute motion in Y and X directions per frame for unregistered and registered images is compared in Figs. 6 and 7, respectively. The mean absolute motion per frame of the heart over all of the data sets decreased from  $5.3 \pm 5.2$  (mean  $\pm$  SD) mm to  $0.8 \pm 1.3$  mm along the Y direction, and from  $3.0 \pm 3.7$  mm to  $0.9 \pm 1.2$  mm along the X direction. Figure 8 gives the average relative errors in flow indices for the eight regions in myocardium before and after registration for all of the 10 patients. An overall mean absolute improvement of 77% in the estimation of perfusion flow indices is observed as compared to those from manual registration. Table 3 summarizes the results of paired *t*-tests with Bonferroni correction. The flow values before and after registration are significantly different.

Registration of two-chamber-view data sets was similar in performance to the short-axis images. In the long-axis data sets the motion is mostly in the vertical

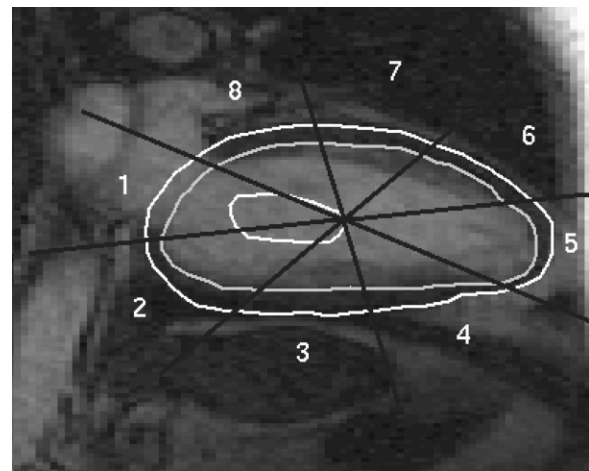


**Figure 10.** The myocardium in the two-chamber-view long-axis data set is divided into regions to estimate the flow indices by performing a two-compartment model analysis for a typical patient. Note that region 1 is blood pool and is not used. The region in the blood pool chosen to compute the input function for estimating the perfusion flow indices is also shown in the center of the LV blood pool.

direction and negligible motion is observed in the horizontal direction (on the order of 1 mm). The results for 10 different long-axis data sets are shown in Figs. 9–11. Figure 9 compares the mean absolute motion over all of the time frames in the vertical or Y direction before and after registration. Significant motion reduction is obtained after registration. Also, the myocardium in each long-axis data set is divided into ROIs as shown in Fig. 10, and perfusion flow indices to the tissue regions are obtained by fitting the time curves of the regions to the two-compartment model. Figure 11 shows the average relative error in the estimation of perfusion flow indices for the long-axis data sets before and after registration by comparing them with those obtained from manual registration. Table 4 shows the results of the paired *t*-tests with Bonferroni correction by comparing the flow indices for the long-axis data sets. We again see that

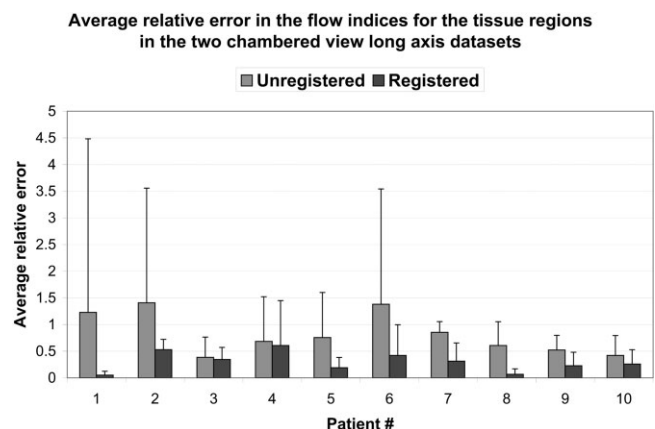


**Figure 11.** Comparison of the average relative error in the flow indices for the eight tissue regions before and after registration for 10 two-chamber long-axis data sets.

Table 4

Comparison of Flow Indices of the Tissue Regions Before and After Registration for the 10 Long Axis Datasets Using Paired *t*-Tests with Bonferroni Correction

Paired <i>t</i> -tests with Bonferroni correction for flow indices	Manually registered vs. unregistered	Iterative model-based vs. unregistered	Manual registration vs. iterative model-based registration
<i>P</i>	0.0117	0.0126	1

model-based registration makes a significant difference in the estimation of the flow indices.

### Time Factor

The algorithm required at most five iterations for the data sets to converge. For our Matlab implementations, the time taken by the iterative model-based method using the linearized model in Eq. [3] to find the optimum parameters for fitting the time curves is three to four times less than that required for a conventional nonlinear least-squares method. The time taken by the algorithm to register a data set with approximately 6000 pixels per frame and 70 time frames is 1.7 minutes per iteration on a Linux machine with an AMD 270 dual core and 4G RAM. This amount of time is not prohibitive for offline processing of cardiac perfusion studies, and could be substantially reduced with optimized implementations.

### DISCUSSION

The iterative model-based method improves registration compared to the more standard mean square difference methods by using model reference images for each frame. The intuitive reasoning is that a single reference frame does not well represent the changing distribution of Gd, and creating reference frames for each time frame can prevent misregistrations of the frames. Another advantage to the use of model-based registration is the inherent denoising by the fitting process. The reduced noise likely contributes to more robust registrations. It is of particular interest that the dynamic image data outside of the LV can be relatively well represented by a two-compartment model with an input function taken from the RV for short-axis data sets, and an input function from the LV for long-axis data sets. This is a new finding that could be applied in other ways, such as for denoising dynamic myocardial perfusion images. Another useful finding is that the model-based approach does not require a large dose of contrast agent. A range of doses were used successfully here, which implies that the method is applicable for most practical doses.

Correction of rotational motion was not addressed in this study; however, the method could readily be extended to handle rotational motion. For the data sets we used there appeared to be negligible rotation motion. Others have corrected for translational and rotational motion and used results obtained from manual registration without rotation as the gold standard (6,8). Bidaut and Vallee (6) reported that the relative motion of the anatomical landmarks at the extremities and center of the mid-wall segment is

reduced compared to manual registration after correction for rotational motion is incorporated.

Performing a comparison with manually shifted images is a good way to determine how well different image registration methods perform. The ideal method is to use task-dependent metrics. For example, in the case of myocardial perfusion images, the flow indices of the tissue when used in diagnosis or prognosis are a more relevant gauge of registration performance. A useful surrogate for the ideal method is to compare perfusion values from the unregistered and registered data, as in Table 2. The flows are not expected to be a sensitive measure of registration. For example, it is possible that even though the heart moves, the same or similar pixel intensities will be shifted into the ROI. However, a comparison of flows is more relevant clinically than a comparison of shifts. Also, image frames with out-of-plane motion can affect the regional flow indices of the tissue. Despite these limitations, there is an improvement in the flow indices calculated with model-based registration in that the values more closely match the results from manually registered data.

In conclusion, model-based registration provides a robust method for estimating in-plane shifts to register DCE myocardial images for short-axis and two-chamber long-axis data sets. In contrast to methods that register all of the image frames to a single reference image, the model-based method provides a unique means of creating a reference image for each time frame. Since many of the time frames bear little resemblance to the single reference image, improved registration can be achieved with the use of model-based registration.

### ACKNOWLEDGMENTS

We appreciate the help of Chris McGann, M.D., Henry Buswell, Melody Johnson, and Nate Pack with data acquisition.

### REFERENCES

- Schwitzer J, Nanz D, Kneifel S, et al. Assessment of myocardial perfusion in coronary artery disease by magnetic resonance: a comparison with positron emission tomography and coronary angiography. *Circulation* 2001;103:2230–2235.
- Al-Saadi N, Nagel E, Gross M, et al. Noninvasive detection of myocardial ischemia from perfusion reserve based on cardiovascular magnetic resonance. *Circulation* 2000;101:1379–1383.
- Bertschinger KM, Nanz D, Buechi M, et al. Magnetic resonance myocardial first-pass perfusion imaging: parameter optimization for signal response and cardiac coverage. *J Magn Reson Imaging* 2001;14:556–562.



4. Vallee JP, Sostman HD, MacFall JR, et al. Quantification of myocardial perfusion by MRI after coronary occlusion. *Magn Reson Med* 1998;40:287-297.
5. Cullen JH, Horsfield MA, Reek CR, Cherryman GR, Barnett DB, Samani NJ. A myocardial perfusion reserve index in humans using first-pass contrast-enhanced magnetic resonance imaging. *J Am Coll Cardiol* 1999;33:1386-1394.
6. Bidaut LM, Vallee JP. Automated registration of dynamic MR images for the quantification of myocardial perfusion. *J Magn Reson Imaging* 2001;13:648-655.
7. Gallippi CM, Kramer CM, Hu YL, Vido DA, Reichek N, Rogers WJ. Fully automated registration and warping of contrast-enhanced first-pass perfusion images. *J Cardiovasc Magn Reson* 2002;4:459-469.
8. Dornier C, Ivancevic MK, Thevenaz P, Vallee JP. Improvement in the quantification of myocardial perfusion using an automatic spline-based registration algorithm. *J Magn Reson Imaging* 2003;18:160-168.
9. Thevenaz P, Ruttimann UE, Unser M. A pyramid approach to sub-pixel registration based on intensity. *IEEE Trans Image Process* 1998;7:27-41.
10. Bracoud L, Vincent F, Pachai C, Canet E, Croisille P, Revel D. Automatic registration of MR first-pass myocardial perfusion images. *Lect Notes Comput Sci* 2003;2674:215-223.
11. Viola P, Wells III WM. Alignment by maximization of mutual information. *Int J Comput Vis* 1997;24:137-154.
12. Stegmann MB, Olafsdottir H, Larsson HBW. Unsupervised motion-compensation of multi-slice cardiac perfusion MRI. *Med Image Anal* 2005;9:394-410.
13. Buonaccorsi GA, Roberts C, Cheung S, Watson Y, Parker GJ. A novel method of model-based rigid registration for dynamic contrast enhanced MRI studies. In: *Proceedings of 13th Annual Meeting of ISMRM, Miami Beach, FL, USA, 2005*. Abstract 742.
14. Tofts PS, Brix G, Buckley DL, Evelhoch JL, et al. Estimating kinetic parameters from dynamic contrast-enhanced T1-weighted MRI of a diffusable tracer: Standardized quantities and symbols. *J Magn Reson Imaging* 1999;10:223-232.
15. Jerosch-Herold M, Swingen C, Seethamraju RT. Myocardial blood flow quantification with MRI by model-independent deconvolution. *Med Phys* 2002;29:886-897.
16. Choyke PL, Dwyer AJ, Knopp MV. Functional tumor imaging with dynamic contrast-enhanced magnetic resonance imaging. *J Magn Reson Imaging* 2003;17:509-520.
17. Murase K. Efficient method for calculating kinetic parameters using T1-weighted dynamic contrast-enhanced magnetic resonance imaging. *Magn Reson Med* 2004;51:858-862.
18. Feng D, Wang ZZ, Huang SC. A study on statistically reliable and computationally efficient algorithms for generating local cerebral blood flow parametric images with positron emission tomography. *IEEE Trans Med Imaging* 1993;12:182-188.